

Source: Cohere Technologies, AT&T, CMCC, Deutsche Telekom, Telefonica, Telstra
Title: OTFS Modulation Waveform and Reference Signals for New RAT
Agenda item: 8.1.4.1
Document for: Discussion and Decision

1. Introduction

The 5G air interface and associated modulation have to support a number of diverse requirements and use cases (e.g., eMBB, high-speed use case, mMTC etc.) as detailed in e.g., [1].

The associated modulation waveform would then have to exhibit high performance in many diverse scenarios of high or low Doppler, delay spread, carrier frequency etc. This is possible if the modulation scheme takes full advantage of the fading multipath nature of the channel and extracts the full diversity present in the channel in all dimensions of time, frequency and space. Such a flexible waveform can serve as an integral part of a flexible air interface and associated core network [2].

In this contribution, we provide a brief introduction to a novel modulation technique we call Orthogonal Time Frequency Space (OTFS) – see also [3]. We will see that OTFS arises as a well suited modulation for the time and frequency selective fading channel. OTFS characterizes the Doppler induced time varying nature of the wireless channel and parameterizes it as a 2D impulse response in the delay-Doppler domain as will be explained later. We study the modulation's performance and hence focus primarily on the eMBB use case. In addition to the OTFS diversity gains mentioned above, we have additional benefits of low reference signal overhead, and enhanced CSI quality and MIMO performance.

There are many areas where an OTFS inspired air interface design can provide benefits to 5G systems. In this short contribution we focus on two main ones: i) the ability to extract the channel capacity and exploit its diversity with reasonable complexity as the number of antennas grows and ii) the ability to design reference signal schemes that multiplex a large number of antenna ports in a dedicated (“pilot”) subgrid of the time-frequency plane. We show performance results with significant performance gains over OFDM for multiple MIMO configurations.

In a nutshell, the OTFS modulation establishes a novel coordinate system to reveal the geometry of the wireless channel. OTFS augments the existing channel model by adding a second dimension representing the Doppler characteristics of each reflective path. In this regard, OTFS captures the exact behavior of the wireless multipath medium in a concise two-dimensional physical representation that is stable and slowly varying compared to the channel's time and frequency variations. OTFS converts the time-varying impulse response to a time independent 2D convolution operation for the duration of the TTI, governed by the geometry (aka location, relative velocity and angle of arrival) of the physical objects in the propagation path. In this way every symbol experiences the full diversity of the channel. Due to its precise, efficient delay-Doppler channel representation OTFS allows the acquisition of the exact coupling between a large number of antennas in the network, setting the ground for beamforming, null steering and scaling with the MIMO order and the number of devices.

2. A 2-D Modulation: from OFDM to OTFS

The development of OFDM modulation typically assumes a slowly varying channel with impulse response $h(\tau, t) \approx h(\tau)$ that is locally independent of the time variable t . Under this assumption and with the addition of a cyclic prefix to the data to ensure the channel effect is a circular convolution, we obtain a multiplicative channel model in the frequency domain

$$Y[m] = H[m]X[m] + V[m] \quad (1)$$

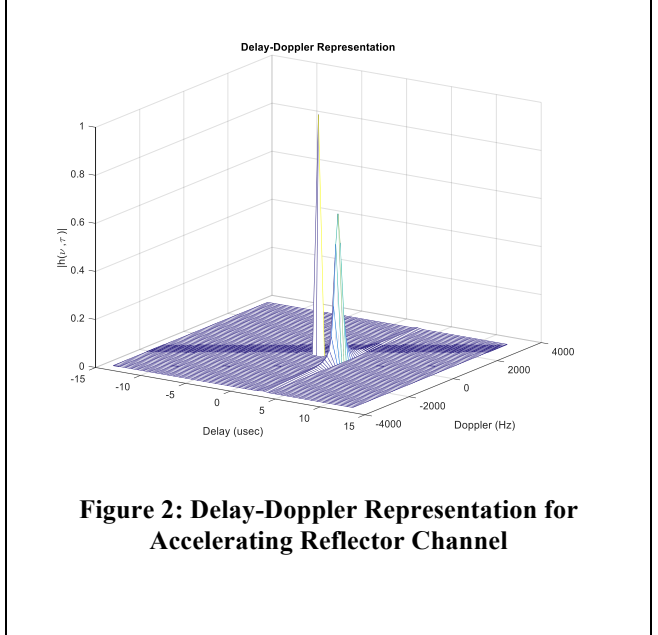
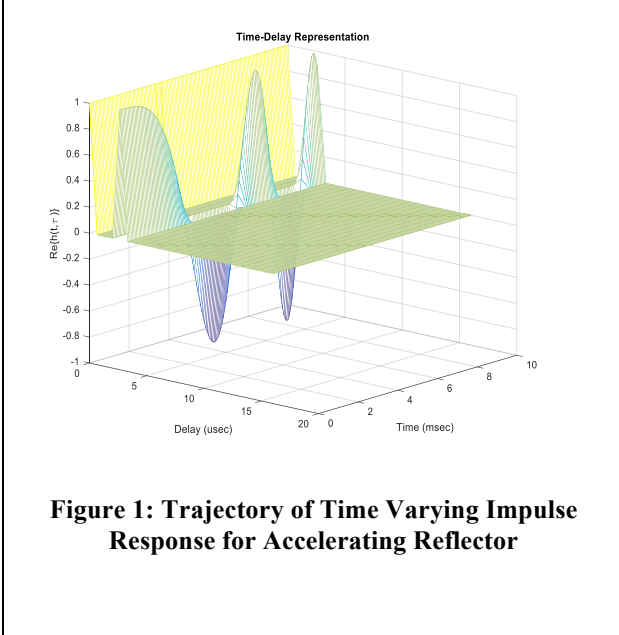
for frequency bins $m = -\frac{M}{2}, \dots, \frac{M}{2} - 1$ where $H[m]$ is the frequency response of the channel evaluated at multiples of the subcarrier spacing Δf . The frequency response is given by

$$H[m] = \int h(\tau) e^{-j2\pi m \Delta f \tau} d\tau \quad (2)$$

In order to develop a modulation scheme suited for the time-frequency fading channel, we need to avoid the time invariance simplification and examine the full effects of the time varying channel on the transmitted waveform. We will abandon the $h(\tau, t)$ time varying impulse response characterization of the channel, which is less useful, and instead parameterize the channel via its delay-Doppler response $h(\tau, \nu)$. In this description, the channel operation on the transmitted waveform $s(t)$ is described by

$$r(t) = \iint h(\tau, \nu) e^{j2\pi \nu (t-\tau)} s(t-\tau) d\nu d\tau \quad (3)$$

The delay Doppler impulse response has an appealing physical interpretation: for every point (τ, ν) the value $h(\tau, \nu)$ represents the reflectivity of a cluster of reflectors sharing these specific delay and Doppler parameter values. The parameterizations $h(\tau, \nu)$ and $h(\tau, t)$ are equivalent and can both describe general time-varying systems (e.g., accelerating reflectors etc.); in fact the two parameterizations are related by an appropriate Fourier transform along the t axis. An example of the two parameterizations for a channel with two reflectors is shown in Figure 2 and Figure 3. The main thing to notice is that the $h(\tau, \nu)$ representation is much more compact than the $h(\tau, t)$ representation as demonstrated in those figures. This fact can be exploited for purposes of channel estimation and equalization.



Using the channel equation (3), we can derive a channel model in the time-frequency domain for the given bandwidth and TTI time duration (of an OFDM system), which explicitly models Doppler effects. It turns out that under some mild assumptions, a multiplicative channel model is obtained

$$Y[n, m] = H[n, m]X[n, m] + V[n, m] \quad (4)$$

for frequency bins $m = -\frac{M}{2} + 1, \dots, \frac{M}{2}$ and time $n = 0, \dots, N - 1$ (measured in OFDM symbols), where N is the total number of OFDM symbols in the TTI. A fundamental observation is that the channel time-frequency response $H[n, m]$ is related to the delay Doppler impulse response $h(\tau, \nu)$ via the following transform¹

$$H[n, m] = \iint h(\tau, \nu) e^{j2\pi \nu n T} e^{-j2\pi m \Delta f \tau} d\nu d\tau \quad (5)$$

where T is the length of the OFDM symbol (plus the cyclic CP extension). Equation (5) can be thought of as a 2D Fourier transform version of the delay-Doppler impulse response $h(\tau, \nu)$ (it is called the Symplectic Fourier Transform in the math community).

¹ The mathematically precise equation is $H[n, m] = \iint [h(\tau, \nu) e^{-j2\pi \nu \tau}] e^{j2\pi \nu n T} e^{-j2\pi m \Delta f \tau} d\nu d\tau$ but typically we absorb the exponential inside the brackets in the definition of the channel response $h(\tau, \nu)$ arriving at the simpler equation in the text.

Based on the channel equations (4), (5), we wish to derive a pre-processing step, which will transform the multiplicative fading channel to a convolution channel that is time independent for the duration of the TTI. To this end, we map the information bearing QAM symbols $x[k, l]$ to the time-frequency symbols $X[n, m]$ via a set of 2D complex exponential basis functions

$$X[n, m] = \frac{1}{MN} \sum_{k=0}^{N-1} \sum_{l=0}^{M-1} x[k, l] b_{k,l}[n, m] \quad (6)$$

$$b_{k,l}[n, m] = e^{-j2\pi(\frac{ml}{M} - \frac{nk}{N})}$$

Looking more carefully at the basis functions $b_{k,l}[n, m]$ we have the following remarks:

- Along the frequency bin dimension m , the basis functions $e^{-j2\pi(\frac{ml}{M})}$ constitute a set of DFT basis function and relate the frequency domain to a new domain we call the delay domain.
- Along the time dimension n , the basis functions $e^{j2\pi(\frac{nk}{N})}$ constitute a set of IDFT basis function and relate the time domain to a new domain we call the Doppler domain.
- In conclusion, the OTFS scheme allocates the information QAM symbols $x[k, l]$ in the delay-Doppler domain; those symbols are subsequently transformed to the familiar time-frequency domain via Eq. (6). The mapping of information symbols to time-frequency basis functions is illustrated in Figure 3.

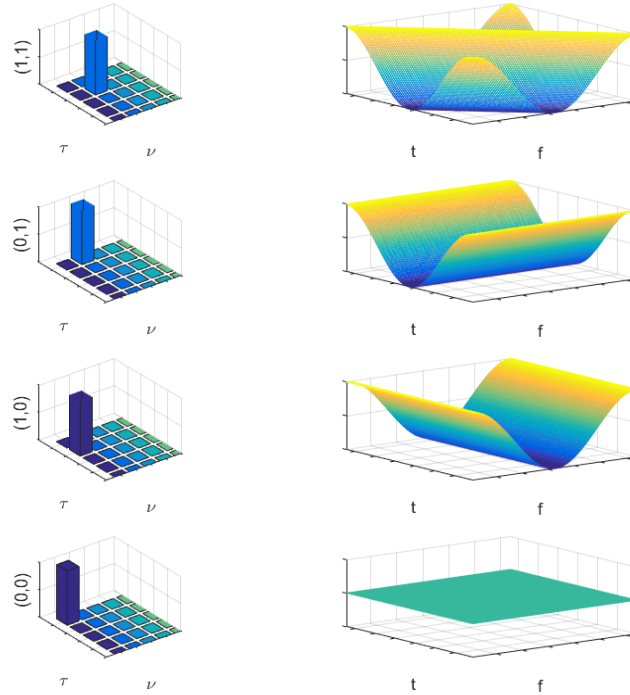


Figure 3: Mapping of Information Symbols (delay-Doppler Domain) to Basis Functions (Time-Frequency Domain)

Notice that the 2D OTFS transform of (6) consists of a DFT along the delay/frequency dimension and an IDFT along the Doppler/time dimension. This is known as a two dimensional Symplectic DFT in the math literature and is needed here to match the nature of the channel response in (3).

In the receiver, the inverse OTFS transform is applied, i.e., the inverse Symplectic DFT on the time frequency data

$$\hat{x}[l, k] = \sum_{m=0}^{M-1} \sum_{n=0}^{N-1} Y(n, m) b_{k,l}^*(n, m) \quad (7)$$

$$b_{k,l}^*(n, m) = e^{j2\pi(\frac{lm}{M} - \frac{kn}{N})}$$

In terms of implementation, the OTFS transform consists of pre- and post-processing blocks in the transmitter and receiver respectively, as depicted in Figure 4. This block diagram is analogous to the pre- and post-processing DFT blocks used to implement SC-FDMA on top of an underlying OFDM signal chain.

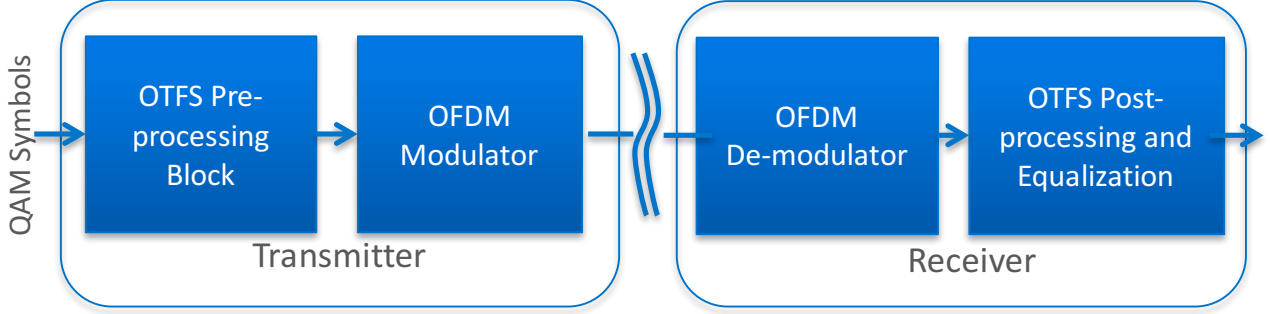


Figure 4: OTFS Architecture with OTFS Transform Pre- and Post-Processing Blocks

It should be noted that the OTFS modulation can also be derived as a pre- and post-processing of multicarrier systems other than OFDM (e.g., filterbank multicarrier); the details of these developments are outside the scope of this paper.

The purpose of the OTFS pre- and post-processing is to enable QAM modulation in the delay-Doppler domain, where all QAM symbols see the same 2D convolution channel and the difficulties associated with time and frequency fading within the TTI are avoided. In particular, it can be shown that the end-to-end channel in the delay-Doppler domain is given by the 2D circular convolution

$$\hat{x}[k, l] \approx \frac{1}{MN} \sum_{m=0}^{M-1} \sum_{n=0}^{N-1} x[n, m] h_w \left(\frac{l-m}{M\Delta f}, \frac{k-n}{NT} \right) + v[k, l] \quad (8)$$

The delay-Doppler impulse response $h_w(\tau, \nu)$ is a continuous 2D circular convolution of the delay-Doppler channel response $h(\tau, \nu)$ with a two-dimensional Dirichlet kernel introduced due to the finite transmission bandwidth and TTI or OTFS frame length

$$h_w(\tau, \nu) = \iint e^{-j2\pi\nu\tau'} h(\tau', \nu') w(\tau - \tau', \nu - \nu') d\tau' d\nu' \quad (9)$$

$$w(\tau, \nu) = \sum_{m=0}^{M-1} \sum_{n=0}^{N-1} e^{-j2\pi(vnT - \tau m\Delta f)} \quad (10)$$

Equation (8) indicates that the end-to-end transmission scheme in the delay-Doppler domain can be thought of as a 2D-convolutive scheme over the whole TTI in both the delay and Doppler dimensions.

Figure 5 illustrates the processing flow of the OTFS transform and the underlying multicarrier system as well as the nature of the channel in the delay-Doppler domain in contrast to the time-frequency and waveform domains. It highlights the multiplicative versus 2D-convolutive nature of the channel in the time-frequency versus delay-Doppler domains respectively.

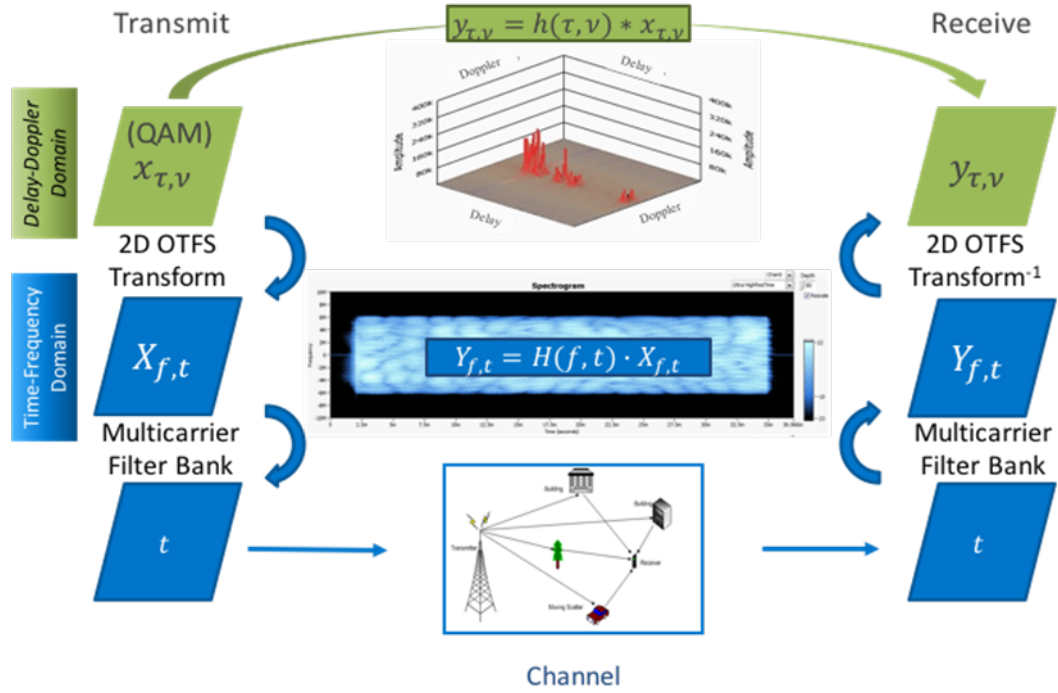


Figure 5: Three Different Views of the Channel in the Waveform, Time-Frequency and Delay-Doppler Domains

This architecture provides the following benefits:

- Resolution of the reflectors in both the delay and Doppler domains, thus extracting the full time and frequency diversity of the channel.
- Transformation of the fading channel in the time-frequency domain to a time invariant channel in the delay-Doppler domain for the duration of the TTI. This time invariance property holds even if the TTI length is larger than the coherence time of the channel.

3. Receiver Architectures and MIMO Processing

Equation (8) provides a blueprint for possible receiver equalizer architectures. Since the channel manifests itself as a 2D circular convolution, receiver architectures borrowed from single carrier OFDM systems can be employed if extended to two dimensions. The simplest receiver is a linear MMSE or ZF receiver, which can be implemented in either the time-frequency or delay-Doppler domains. Higher performance can be obtained with more advanced receivers including decision feedback equalizers (DFE) and turbo equalizers. In general, the topic of detailed complexity and performance comparisons of different receiver architectures is outside the scope of this introductory contribution. This brief section is intended to mostly introduce different possible receiver architectures and only touch upon complexity questions.

In the case of MIMO systems, Equation (8) generalizes to a matrix 2D circular convolution, enabling the adaptation of a number of different MIMO architectures like linear MMSE, multichannel DFE, SIC, and approximate maximum likelihood (ML). In terms of complexity and if we focus on the SISO case, the linear MMSE receiver is the least complex and is similar to the complexity of the OFDM MMSE receiver. The DFE receiver consists of a feedforward part, with complexity equivalent to the linear MMSE receiver, and an additional feedback part tightly coupled with a detector. This translates to some additional complexity compared to a linear OFDM receiver.

In the MIMO case the complexity comparison is not that straightforward. A multichannel DFE is still more complex than a linear MMSE, but when compared with nonlinear OFDM receivers like SIC and ML, the DFE receiver may get reasonably close to capacity with less complexity than an ML OFDM receiver (especially for high order MIMO).

4. OTFS Framework for Antenna Port Reference Signal Multiplexing

Reference signals (RSs) are typically placed in the time frequency domain to assist the receiver in estimating the channel, often in coarse (regular or irregular) grid throughout or beyond the TTI. Often in OFDM systems multiple antenna ports are multiplexed on the same coarse grid using different (ideally orthogonal) signature sequences on the coarse RS grid points (e.g., using Hadamard codes or Zadoff-Chu sequences). Understanding the effects of the channel in the delay-Doppler domain can lead us to a better way of multiplexing antenna port RSs either in the time-frequency or the delay-Doppler domains. In fact, significant improvements in the RS overhead can be achieved when multiplexing a large number of antenna ports.

Assume that the RSs are placed in a coarse grid of every N_0 symbols and every M_0 subcarriers. For example, in the uplink the SRSs can be placed on a grid with $N_0 = 14$ and $M_0 = 1$ for a spacing of 1 msec between successive SRS symbols, as shown by the red dots in Figure 6, resulting in a reference signal overhead of around 7%. The data portion of the time-frequency grid is shown by the green circles.

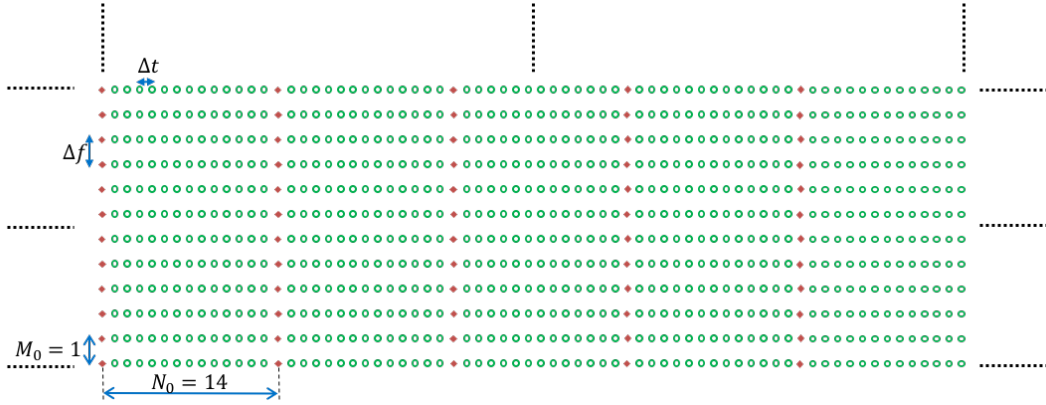


Figure 6: Time-Frequency Reference Signal Grid.

Notice that the multiplicative channel equation still holds in this coarse RS grid

$$Y_p[nN_0, mM_0] = H[nN_0, mM_0]X_p[nN_0, mM_0] + V[nN_0, mM_0] \quad (11)$$

hence, taking a RS frame in the coarse grid of M_p RS subcarriers times N_p RS symbols we can define a RS time-frequency and associated delay-Doppler frame. For example, in the case of SRSs, we can have $M_p = 600$ subcarriers (for a 10 MHz system) times say $N_p = 5$ SRS symbols spaced 1 msec apart for a 5 msec RS observation window.

If we wish to multiplex multiple antenna ports in this coarse RS grid, we have to consider the design of (preferably orthogonal) multiplexing RS sequences. This design is typically considered in the time-frequency domain but it equivalently can be done in the delay-Doppler domain where the characteristics of the channel are more readily apparent. As an illustration, Hadamard codes in the time-frequency domain have been used in UE specific RSs, which intuitively makes sense due to their orthogonality. However, this orthogonality is lost after the channel effects. The question here is how to design orthogonal RS sequences which approximately maintain their separation or orthogonality after the channel effects.

Recall that the channel equation of (11) holds for the RS subgrid, and therefore the equivalent channel equation in the delay-Doppler domain is given by

$$\hat{x}_p[k, l] \approx \frac{1}{M_p N_p} \sum_{m=0}^{M-1} \sum_{n=0}^{N-1} x_p[n, m] h_w\left(\frac{l-m}{M_p M_0 \Delta f}, \frac{k-n}{N_p N_0 T}\right) \quad (12)$$

This convolution equation reveals that the effects of the channel are local, that is a delta in the delay-Doppler domain will be spread only to the extent of the support of the channel in the delay and in the Doppler dimensions. This fact provides the blueprint for multiplexing antenna ports in this domain, i.e., represent each antenna port sequence as an RS impulse, and space the impulses apart sufficiently, so that when the impulses are spread by the channel they still do not overlap or overlap minimally. Figure 7 shows an example of such an arrangement of RS antenna ports in the delay-Doppler domain. Notice that each antenna port RS in Figure 7 is generally affected by a different channel.

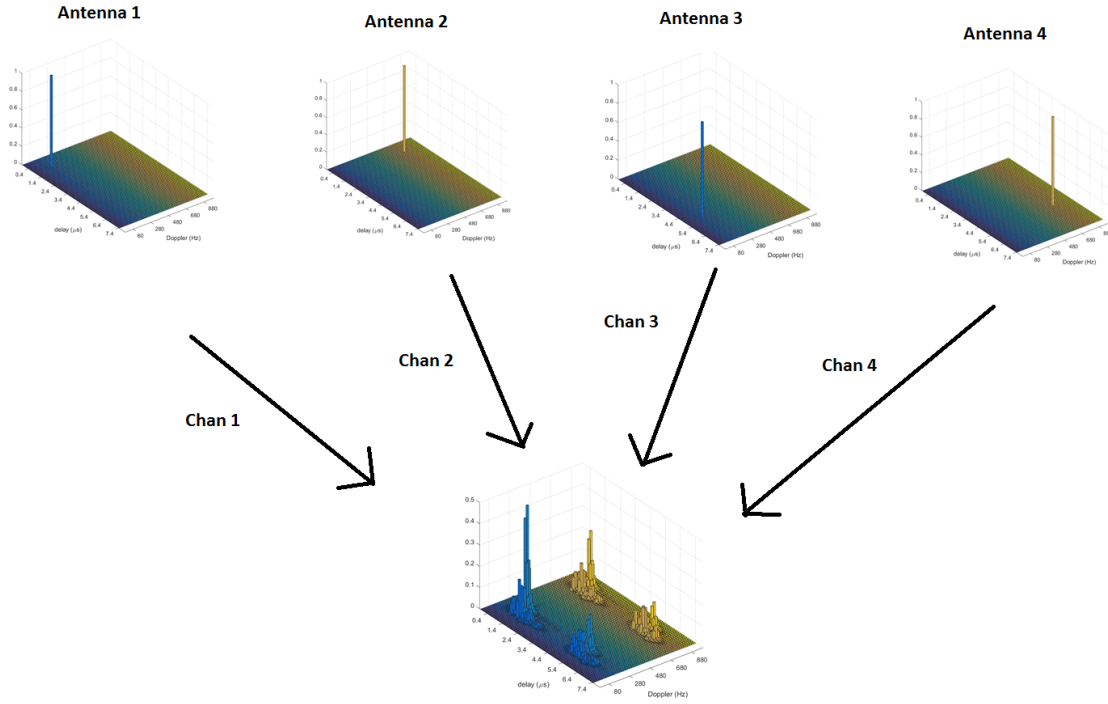


Figure 7: Antenna Ports Multiplexed in the delay-Doppler Domain

Equivalently, each one of the deltas in the delay-Doppler domain corresponds to a two-dimensional complex exponential on the coarse grid of the time-frequency domain. In this way, these RS sequences can be thought of as two dimensional extensions of the Zadoff-Chu sequences.

The number of antenna ports that can be supported simultaneously in the delay –Doppler plane is affected by the following parameters (see Figure 8):

- Delay and Doppler spreads of the channels
- The size of the delay-Doppler plane. If the resolution of the RS grid in the time-frequency domain is $N_0 T \times M_0 \Delta_f$, then the size (span) of the associated delay-Doppler plane is $1/M_0 \Delta_f \times 1/N_0 T$. As an example, if the RS grid is $N_0 T \times M_0 \Delta_f = 1ms \times 15kHz$ then the size of the associated delay-Doppler plane is $66.67\mu s \times 1kHz$.
- The size of the receiver observation window in both time and frequency dimensions (see Figure 9). The observation window in the time-frequency plane induces a convolution with a Dirichlet kernel, increasing the energy of the received RS beyond its delay and Doppler spreads. As a result, a larger observation window will improve the RS packing.

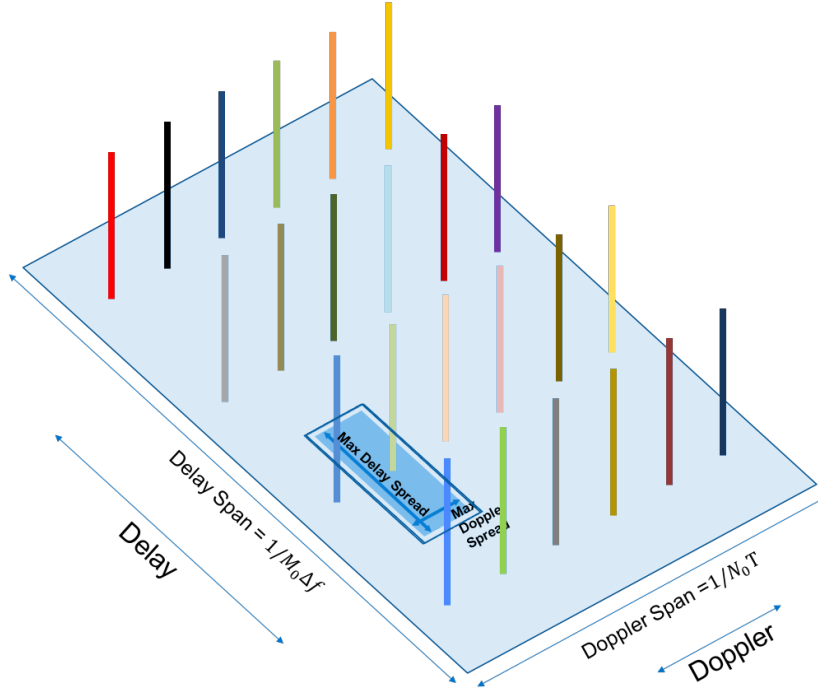


Figure 8: An example of packing 24 RSs in the continuous delay-Doppler plane. The dark shaded area shows the maximum delay and Doppler spreads of a channel, and the solid line around the shaded area shows the additional area assigned to handle the observation window.

For best estimation of the channel response, the reference signal of each antenna port has to occupy an area in the delay-Doppler plane with dimensions of at least the delay and Doppler spreads of its channel. If all the channels have the same delay and Doppler spreads Δ_τ and Δ_ν respectively, and the delay and Doppler spans of the delay-Doppler plane are C_τ^P and C_ν^P respectively, then the maximum number of RSs that can be supported is given by $N_{\max_\tau}^P \cdot N_{\max_\nu}^P$ where $N_{\max_\tau}^P$ and $N_{\max_\nu}^P$ are given by:

$$\begin{aligned} N_{\max_\tau}^P &= \lfloor C_\tau^P / \Delta_\tau \rfloor \\ N_{\max_\nu}^P &= \lfloor C_\nu^P / \Delta_\nu \rfloor \end{aligned} \quad (13)$$

As an example, for ETU-50 channels ($5\mu\text{s}$ delay spread and 50Hz maximum Doppler) and RS grid with resolution $1\text{ms} \times 15\text{kHz}$, the maximum number of RSs that can be supported is $\lfloor 66.67/5 \rfloor \cdot \lfloor 1000/100 \rfloor = 13 \cdot 10 = 130$. This number assumes an infinite observation window. With a finite observation window (limited channel bandwidth and length of time collecting RSs samples) the actual number will be lower but still significant – for example, $11 \cdot 8 = 88$. Note that these 88 multiplexed RSs occupy only 7% of the available throughput, thus the overhead per RS or antenna port is $7\%/88 = 0.08\%$ - significantly lower than currently supported in LTE. As another example, to support ETU-300, it can be shown that in a 10 MHz channel at least 10 RSs can be supported in the delay dimension with low enough channel estimation MSE to support high constellations. This corresponds to an overhead per RS of 0.7%.

Separating the RSs from the data allows for increasing the RS observation window in time, enabling the packing of a larger number of RSs in the Doppler dimension. Note that the large observation window doesn't introduce latency in the processing of the data. As shown in Figure 9 the receiver collects a history of RS samples and when the data arrives it uses the RS history plus the next RS sample following the data to estimate the channel and receive the data.

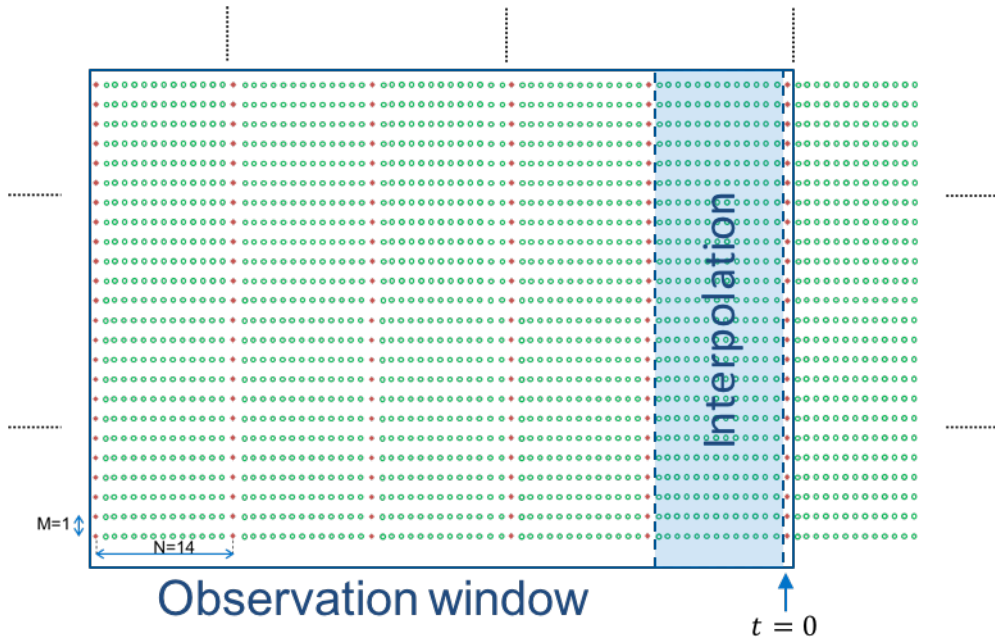


Figure 9: Time-Frequency observation window example. Red points represent the RS grid and green points represent the data grid

Packing the RSs in the delay-Doppler plane has multiple advantages, including:

- Ability to support channels with different delay and Doppler spreads by separating the RSs in the delay-Doppler plane with minimum distances required to support the delay and Doppler spreads of each channel. Figure 10 shows an example of different distances between RSs in the delay-Doppler plane.
- More flexibility in packing the RSs, as the RSs can be placed anywhere in the continuous delay-Doppler plane as opposed to the finite grid selection available in the time-frequency plane.

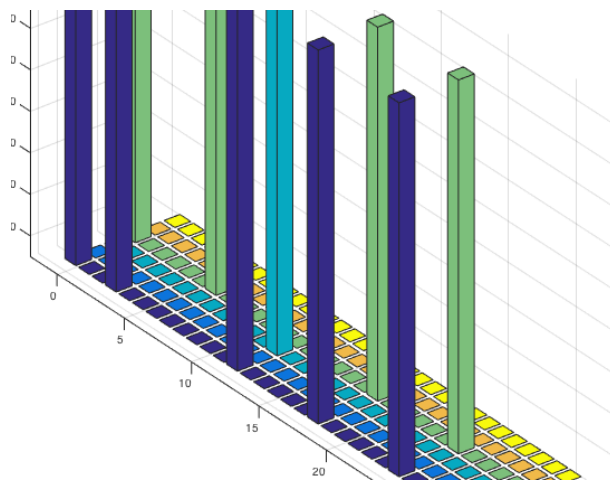


Figure 10: Positioning of RSs with different delay and Doppler spreads in the delay-Doppler plane

5. Performance Results

In this section we present some simulation results to illustrate the performance of an OTFS system. We compare with an OFDM system with the same PHY parameters (BW, subcarrier spacing etc.) and the same FEC coding. We evaluate the performance in the ETU-300 Doppler channel and the EVA-70 channel. We show results for 1x1, 2x2, 4x4 and 8x8 MIMO with CSIR.

The details of the simulation parameters are summarized in Table 1.

Table 1: Link Level Simulation Parameters

Parameter	Value
Subcarrier spacing	15 KHz
Number of subcarriers	600
Bandwidth	10 MHz
Multipath model	EVA, ETU
Max Doppler	70, 300 Hz
Transmission Time Interval length	1 msec
Transmission scheme	2x2, 4x4 MIMO-TM3
FEC Coding	Turbo (LTE)
Precoding	TM3 for OFDM; identity for OTFS
Channel estimation	Ideal
Equalization	Genie aided MMSE-SIC and DFE

The performance for both systems is compared in ideal conditions to provide an indication of the potential performance. Ideal channel estimation and genie aided equalization are used for both OFDM and OTFS simulations. MMSE equalization with genie aided successive interference cancellation is used for OFDM based on the ideal channel, while MMSE-DFE is used for OTFS in the delay-Doppler domain with no error propagation based on the ideal channel. We use the rate 1/3 Turbo code used in LTE for both systems but we relax the packet size constraints/quantization to get identical code rates for both systems. We also map one codeword per layer for both systems. We use identity precoder for the OTFS simulation and we use TM3 precoder for the OFDM 1x1, 2x2, and 4x4 simulations and identity precoder for the 8x8 simulation.

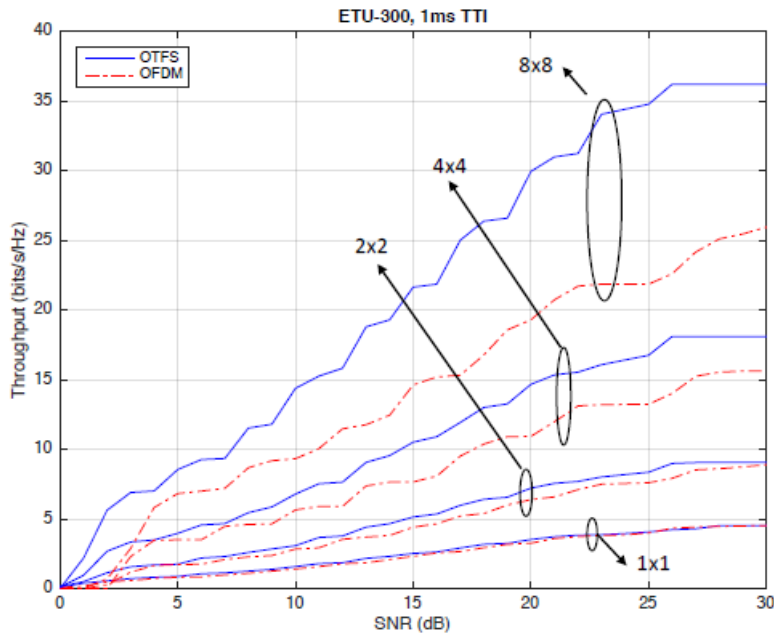


Figure 11: OTFS vs OFDM Comparison for ETU-300 with for 1x1, 2x2, 4x4 and 8x8 MIMO

The performance comparison is illustrated in Figure 11 in terms of throughput versus SNR. For each SNR point, the throughput for all MCSs is estimated by simulation and the maximum one is plotted. This plot is meant to capture the performance of an open loop MIMO system with slow adaptation where only average CQI is fed back to the transmitter. Notice the superior performance of OTFS, which grows as the MIMO order grows.

Figure 12 shows the performance for the same conditions plotted as throughput per stream versus SNR.

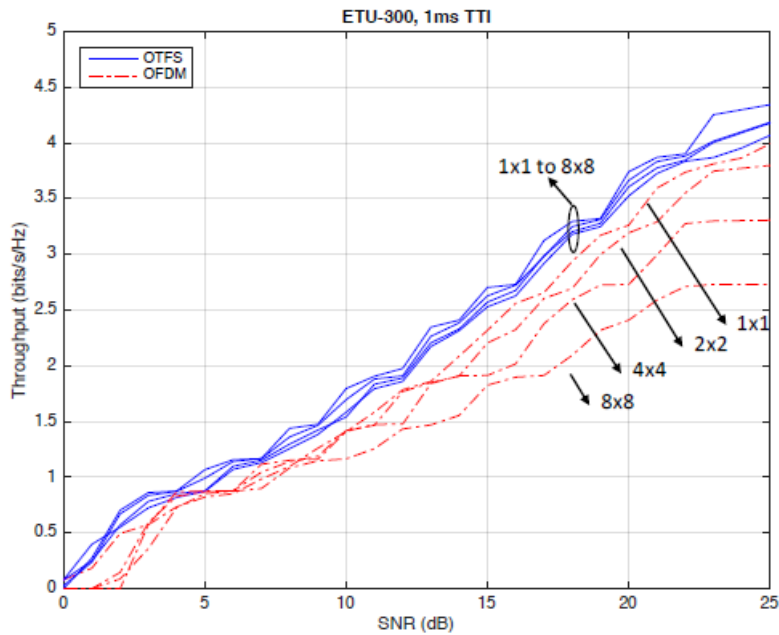


Figure 12: Throughput per Stream OTFS vs OFDM Comparison for ETU-300 for 1x1, 2x2, 4x4 and 8x8 MIMO

Figure 13 and Figure 14 show performance for the EVA-70 channel as total throughput and throughput per stream, respectively. Notice that similar or greater performance gains are seen in this channel as well.

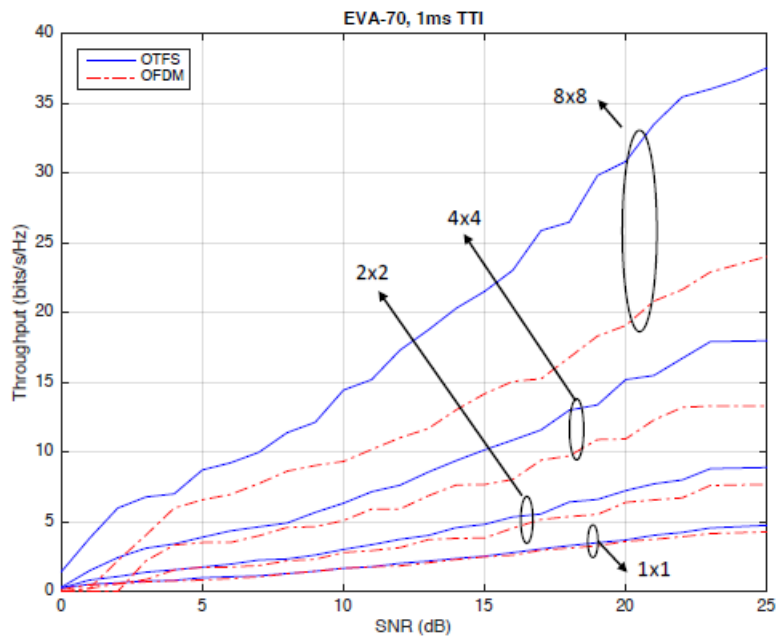


Figure 13: OTFS vs OFDM Comparison for EVA-70 with for 1x1, 2x2, 4x4 and 8x8 MIMO

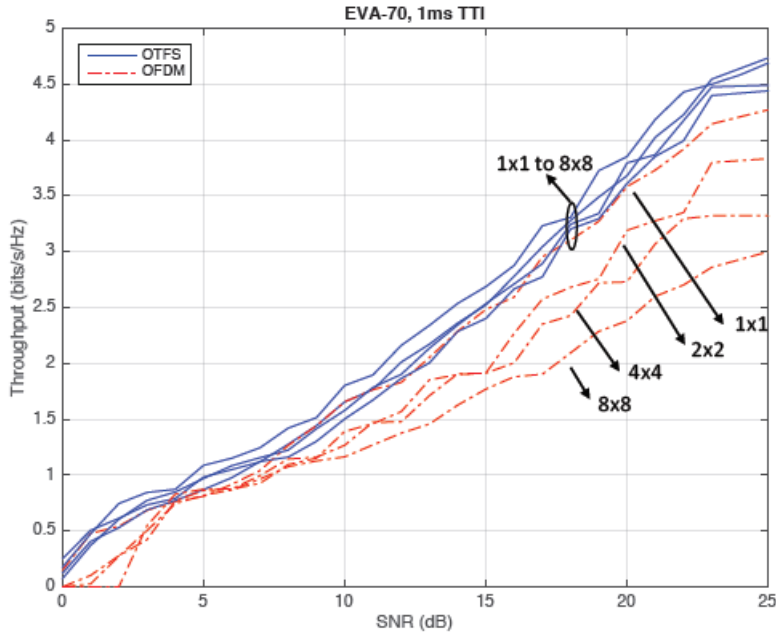


Figure 14: Throughput per Stream OTFS vs OFDM Comparison for EVA-70 for 1x1, 2x2, 4x4 and 8x8 MIMO

In the next simulation we study the performance of OTFS as a function of codeblock size. Figure 15 shows BLER SISO performance for the EVA-200 channel, when the codeblock size is limited to 500, 1000 and 2000 bits. LTE CQI index 9 was used in this simulations (16 QAM, rate 0.6). Notice that the OTFS performance does not depend on the codeblock size, but the OFDM performance is negatively affected, when the codeblock size gets smaller. This is because in the OTFS case all codeblocks experience the full diversity of the channel across the whole TTI, while in the OFDM case smaller codeblocks only occupy a small portion of the time-frequency plane and experience a smaller degree of diversity. In fact, in OTFS transmission every QAM symbol in the delay-Doppler plane experiences the same SNR which is equal to the geometric mean of the channel SNR across time and frequency.

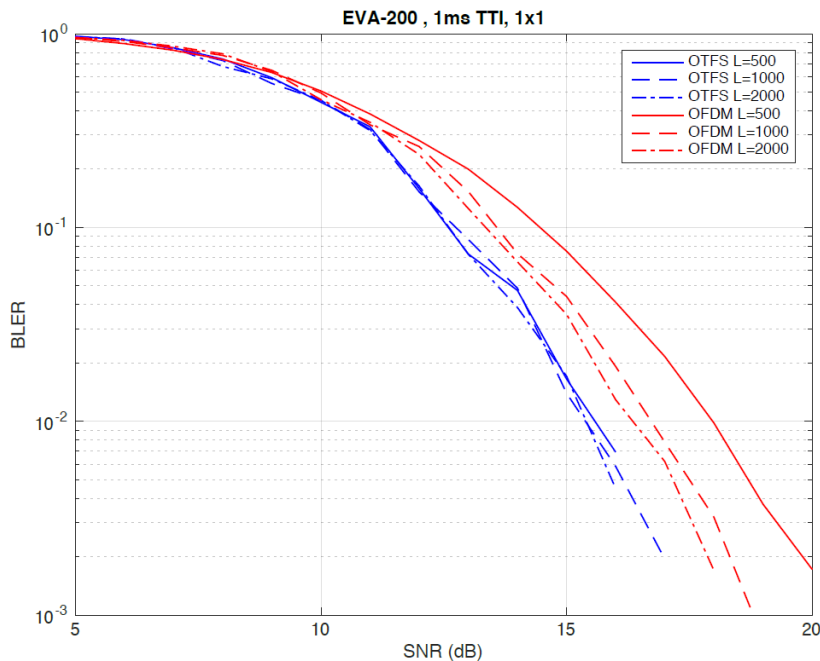


Figure 15: BLER SISO Performance for Codeblock Size of 500, 1000, and 2000 Bits (EVA-200)

This phenomenon is more pronounced in high Doppler scenarios, for example in the high speed train deployment scenario. Figure 16 shows the same results for an EVA-600 channel. Notice the increased diversity gain for the OTFS system in that case.

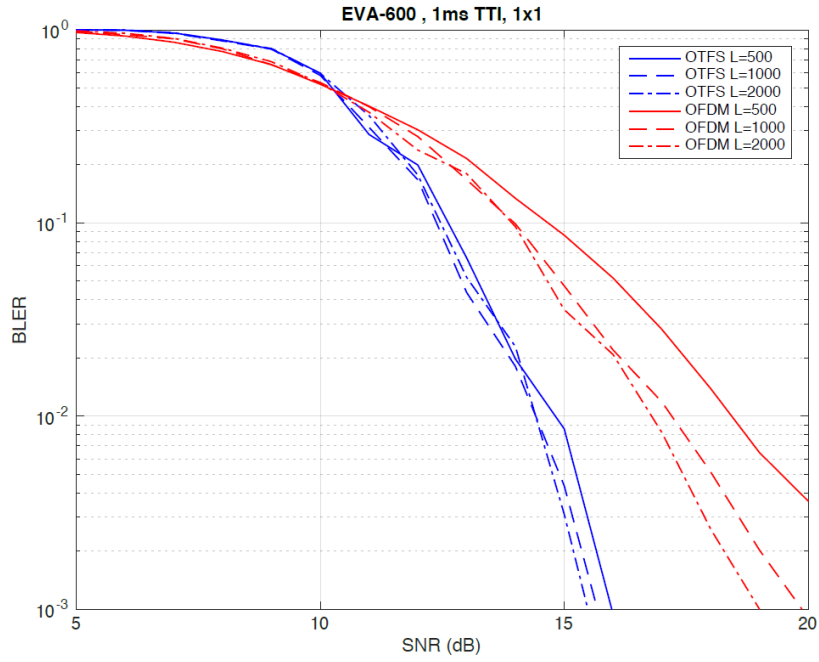


Figure 16: BLER SISO Performance for Codeblock Size of 500, 1000, and 2000 Bits (EVA-600)

Next, we evaluate the impact that the genie aided equalizer may have on the results compared with a non-genie aided equalizer. We have chosen the genie aided DFE (no error propagation) for the OTFS system in order to avoid a full analysis of various receiver architectures in terms of performance and complexity which is outside the scope of this paper (we have similarly used a genie aided SIC for OFDM). However, the performance of the genie aided DFE should not be assumed to be optimistic compared with the performance of advanced receivers. In Figure 17, we compare the performance of the genie aided DFE with a non-genie aided frequency domain turbo equalizer for a 2x2 and a 4x4 system. As can be seen in the figure, the turbo equalizer actually outperforms the genie aided DFE.

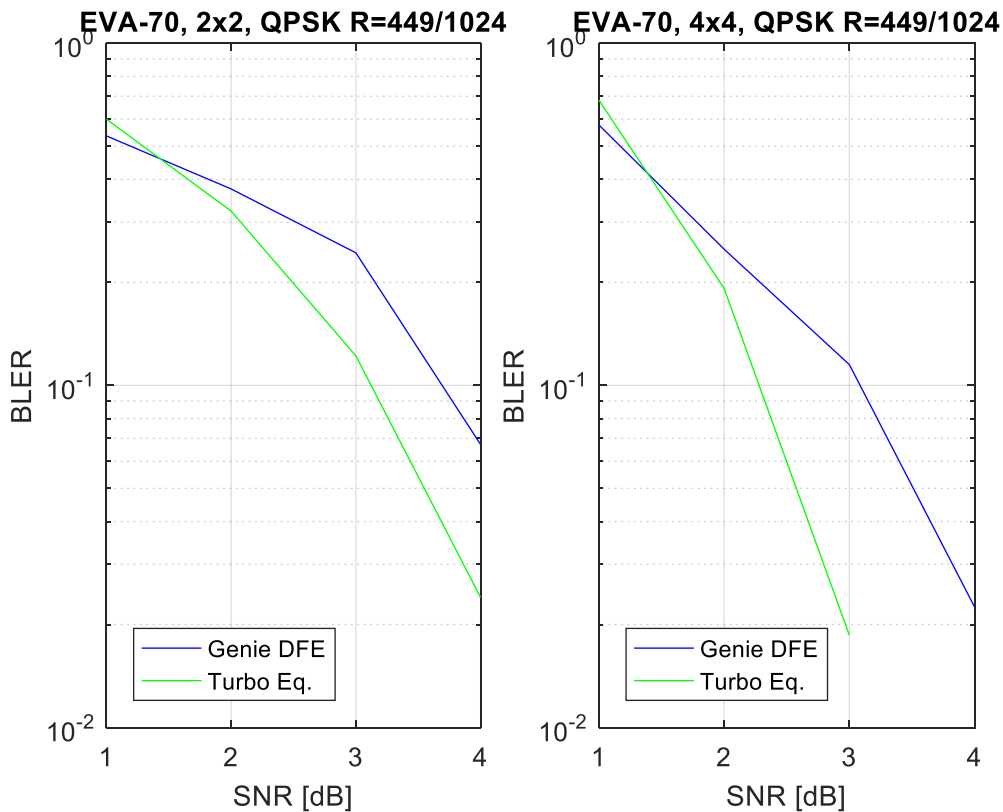


Figure 17: BLER Performance of DFE vs Turbo Equalizer

Next we turn our attention to the simulation of channel estimation performance. The RSs supporting multiple antenna ports were simulated using the parameters in Table 2.

Table 2: Reference Signals Simulation Parameters

Parameter	Value
Subcarrier spacing	15 KHz
Number of subcarriers	600
Bandwidth	10 MHz
Multipath model	ETU
Max Doppler	300 Hz
Pilot grid ($\Delta_t \times \Delta_f$)	1ms x 15KHz
Observation window	600 subcarriers (10 MHz) by 11 time samples (10 ms)
Number of antenna ports	10
Packing (delay x Doppler)	10x1

Figure 18 shows the MSE performance of the channel estimation of one of the channels after receiving the sum of the 10 RSs, each going through a separate (uncorrelated) channel.

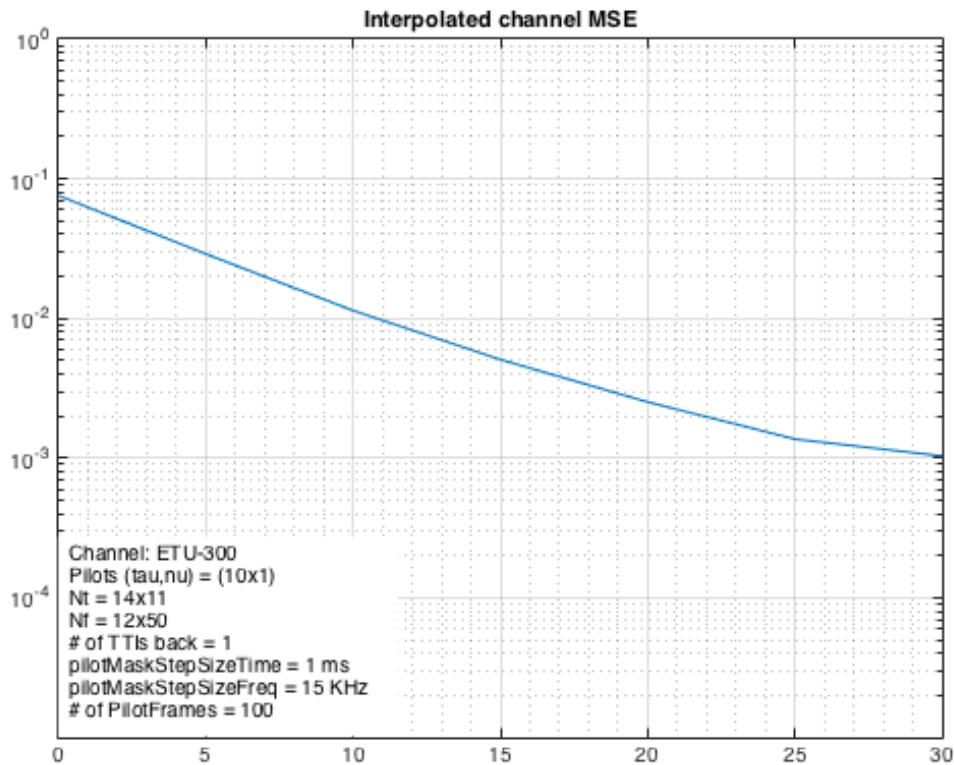


Figure 18: Interpolated channel MSE as a function of channel SNR

6. Conclusion

The delay-Doppler domain provides a novel view of the effects of the wireless channel and points to significant benefits when modulating information symbols in that domain. In particular, the wireless fading channel response becomes a two dimensional time invariant convolution response. All QAM symbols see the same static channel response throughout the transmission interval and extract the maximum diversity of the channel in both the time and frequency dimensions. Significant performance improvements are seen for various MIMO configurations in high Doppler scenarios.

The delay-Doppler domain is also suitable for designing RS sequences for multiplexing a large number of antenna ports with reduced RS overhead. This can result in significant RS overhead improvements for massive MIMO systems.

Proposal: It is requested that the OTFS modulation and reference signal multiplexing scheme is thoroughly evaluated on its merits for the air interface of 5G systems and included in the Technical Report TR38.8XX “TR for Study on New Radio Access Technology Physical Layer Aspects”.

7. References

- [1] TR 38.913, “Study on Scenarios and Requirements for Next Generation Access Technologies”.
- [2] C.-L. I, S. Han, Z. Xu, S. Wang, Q. Sun, and Y. Chen, “[New Paradigm of 5G Wireless Internet](#),” [IEEE Journal on Selected Areas in Communications](#), vol. 34, no.3, pp.474-482, 2016
- [3] R1-162929, “Overview of OTFS Waveform for Next Generation RAT,” Source: Cohere Technologies